Journal of Fluorine Chemistry 130 (2009) 53–60

Contents lists available at ScienceDirect

Journal of Fluorine Chemistry

journal homepage: www.elsevier.com/locate/fluor

XAFS analyses of molten metal fluorides

Haruaki Matsuura [a,b,c,*], Sou Watanabe [a,1], Hiroshi Akatsuka [a], Yoshihiro Okamoto [d], Ashok K. Adya [e]

[a] Research Laboratory for Nuclear Reactors, Tokyo Institute of Technology, 2-12-1-N1-10, Ookayama, Meguro-ku, Tokyo 152-8550, Japan
[b] Conditions Extrêmes et Matériaux: Haute Température et Irradiation, 1D avenue de la recherche scientifique, 45071 Orléans, cedex 2, France
[c] le STUDIUM, Institute for advanced studies in region centre, 3D avenue de la recherche scientifique, 45071 Orléans, cedex 2, France
[d] Japan Atomic Energy Agency, Kansai Photon Science Institute, Kouto 1-1-1, Sayo-cho, Sayo-gun, Hyogo 679-5148, Japan
[e] Condensed Matter Group & BIONTH Centre, School of Contemporary Sciences, University of Abertay Dundee, Bell Street, Dundee DD1 1HG, UK

ARTICLE INFO

Article history:
Received 12 March 2008
Received in revised form 1 July 2008
Accepted 3 July 2008
Available online 23 July 2008

Keywords:
Molten metal fluoride
Rare earth metal fluoride
Alkaline-earth metal fluoride
Lead fluoride
X-ray absorption fine structure
Pyrochemical treatment
Molten salt reactor
Local structure analysis
Synchrotron radiation

ABSTRACT

X-ray absorption fine structure studies of molten metal fluorides containing the materials related to nuclear engineering are intensively summarized. By using XAFS spectra data of divalent and trivalent cation metal fluorides in molten state which have been collected by authors' group for a few years, local structure have been extracted and discussed systematically in conjunction with other spectroscopic studies and numerical calculations. In molten divalent fluorides, tetrahedral coordination of fluorides around a cation is predominant. In the case of pure molten trivalent fluorides, structure with more than 6-coordination has been suggested in some cases, but octahedral coordination structure is much stabilized at heavier rare earth metal fluorides. By mixing with alkali metal fluorides, it is a general trend that inter-ionic distances keep constant, but coordination number of fluorides decreases. In experimental chapter, all the details of sample preparation, furnace installation, X-ray optics setups and data analyses procedures are explained. Finally, future expectations of XAFS technique are also suggested.

1. Introduction

1.1. Molten metal fluoride in nuclear engineering: its brief history

Molten metal fluorides have often been utilized as media in pyro-metallurgic processes. One of the successful industrial processes is aluminium metallurgy. Also in nuclear technology, molten fluorides have attracted many interests. One of which is to apply for liquid fuel reactor system, e.g., molten salt reactor. This concept was proposed by Oak ridge national laboratory, and in practice, molten salt reactor experiment was performed successfully in 1960s. Unfortunately, this project was abandoned soon, but in the beginning of 2000s, molten salt reactor was selected to be developed as one of promising fission reactor candidates in Generation IV programme [1]. Compared to fission reactors using solid fuel, fuel recycle process would be rather simpler. However, a liquid fuel cleaning by metallic extraction of multi-processes is required to remove accumulated fission products and/or corrosion materials. Electrochemical methods depending on elements would be considered to be introduced.

Another possibility in the application of molten fluorides is pyrochemical reprocessing of nuclear fuels from fission reactors. Pyrochemical process has an advantage of compactness, and it leads to reduce secondary wastes evolved from treatment. At the moment, there is no concept using only molten fluorides from the beginning to the end of nuclear treatment processes, but its specific feature of completely different ordering of redox potential referring to that of molten chloride would evolve innovative concept. The processes by adding certain amounts of fluorides into molten chlorides have been examined to be applying to electrochemical treatment of spent nuclear fuels [2].

On the contrary to the wide application to fission reactor systems, there are quite a few examples applied to molten salt technology in the nuclear engineering field, one of which is molten fluoride system used as a blanket candidate in fusion reactors. Molten salt is utilized as a coolant as well as a tritium breeder medium. Historically, Flibe has mainly been considered to be used [3], but $LiF–PbF_2$ is also an alternative candidate in fusion reactor [4].

* Corresponding author at: Research Laboratory for Nuclear Reactors, Tokyo Institute of Technology, 2-12-1-N1-10, Ookayama, Meguro-ku, Tokyo 152-8550, Japan. Tel.: +81 3 5734 3076; fax: +81 3 5734 3379.
E-mail address: hmatsuur@nr.titech.ac.jp (H. Matsuura).
[1] Present address: Japan Atomic Energy Agency, Tokai Research and Development Center, Nuclear Fuel Cycle Engineering Institute, 4-33 Muramatsu, Tokai-mura, Naka-gun, Ibaraki 319-1194, Japan.

0022-1139/$ – see front matter © 2008 Elsevier B.V. All rights reserved.
doi:10.1016/j.jfluchem.2008.07.012

Another application of molten salt is used as incineration media of radioactive materials at an accelerator driven system [5]. In this concept, the advantageous characteristics of large solubility of incinerated elements and good chemical resistance from irradiation can be utilized.

1.2. Several tasks for materialization of chemical processes using molten fluorides

The main problem of molten fluorides is strong corrosive nature, thus oxides should be avoided to be used as any material directly contacted. Because of this reason, the materialization using molten fluorides for industrial processes has been regarded to be difficult, but according to accumulation of several experiences in using fluorides, Ni-based alloys, refractory metals, glassy carbon, boron nitride and oxide-free ceramics, e.g., SiC and AlN are considered to have enough stabilities to the reaction with molten fluorides. However, to apply to nuclear technology process, these materials are kept under irradiated condition, thus in several cases, the development of multi-composite material would be required.

Molten salt is a typical model of liquids where coulombic interaction is predominant, thus compared with water and organic solutions, the numerical examination study would be much easier performed. Once the global model is constructed, it is easy to simulate the chemical behavior of species in experimentally difficult systems, since local structures and dynamic properties related to directly chemical engineering parameters in the processes should be highly correlated. However, compared with molten chlorides, structural information of molten fluorides has still been relatively limited. According to recent innovation of the investigation tools as well as accumulated experiences of handling materials, several publications appear in this decade.

1.3. Spectroscopic studies

Classical infrared and ultraviolet–visible spectroscopic techniques have been well utilized at evaluation of chemical species in liquids. In the case of molten fluorides, as mentioned above, these techniques are extremely difficult, since oxide glasses as optical windows are impossible to be used. Probably these techniques are applicable if either the samples in multi-component fluorides at reduced temperature or the samples containing less concentration of fluoride can be prepared.

Raman spectroscopy is frontier technique in the investigation of molten fluorides. Classically Oak ridge national laboratory performed it to obtain the spectra [6]. Since Belgian group designed carbon windowless cell, a lot of publications have appeared until now [7]. Greek group has published a lot of systematic investigations [8]. Raman spectroscopy is an excellent tool to investigate strong covalent interacted liquids, such as network-like structure, but when more than two contributions of species are overlapped in the spectra, it is very difficult to identify each contribution. If we would expect to obtain the spectra in high resolution, the concentration focused should be enough to be observed, ca. more than 5 mol% of composition of the molten mixture systems. Referring to crystal structure of known solid phase, several species can be conjectured to exist in molten state, however, the information obtained is global, and main discussion can be done by how is the difference from symmetrical structure.

Nuclear magnetic resonance (NMR) spectroscopy is also an excellent tool of the investigation on molten fluoride, since the chemical shifts of ^{19}F and ^{139}La nuclei are very sensitive to the variation of local environment. French group has special probes only adapted to high temperature samples [9]. In this measurement, the samples confined in boron nitride crucible are heated by CO_2 laser heating system. An advantage of this technique is to look at local environment around focused atom in variety of compositions and compounds at various temperatures. But the structural information can be discussed by referring to the chemical shift values of crystal structures already known, and some nuclei which do not depend on the variation of local environment, e.g., ^{7}Li have been empirically recognized and some rare earth nuclei are difficult to be observed by NMR because of their paramagnetic characteristics.

X-ray absorption fine structure (XAFS) can be applied to various compounds and conditions to elucidate the local structure around a given atom. Its great advantage from other techniques is to be possible to derive concrete values of structural parameters, such as inter-ionic distances, coordination numbers and temperature factors, etc. [10]. French and Japanese group independently have developed how to materialize measurements on molten fluorides using synchrotron radiation X-rays. The advantage of XAFS is its flexibility on sample environment, but of course, there are limitations. This technique is mainly applied to the elements heavier than Sc, because of the energy range of X-ray. Historically, the analytical procedure tends to contain human's artifacts and model dependence.

In this review, we focus on XAFS studies on molten fluoride. First, we show some results of molten divalent and trivalent cation metal fluorides and their mixtures with alkali metal fluorides, and compare with the structural parameters obtained each other, referring to the information derived by the other spectroscopic investigations. Second, we explain experimental configuration and data treatment in details to show how we try to avoid human's artifact from analytical procedure. Lastly, the perspective of this research and the way to combine with other techniques are described.

2. Divalent cation metal fluorides and their mixtures

2.1. PbF_2 and LiF–PbF_2 mixture

Molten LiF–PbF_2 has been proposed for application to an alternative candidate as the liquid blanket material for fusion reactor systems [4]. Also, the specific characteristics that pure PbF_2 undergo phase transition from orthorhombic (α) to cubic (β) at 589 K and cubic (β) to superionic phase at 711 K below its melting point (1128 K) [11], would attract much interests from engineers to develop ionic sensor materials. Thus, XAFS spectra of both pure PbF_2 and LiF–PbF_2 at various temperatures have been collected to investigate local structural variation [12] and concentration dependence of LiF–PbF_2 mixtures [13] have also been examined.

The most difficulty of this system was how to treat multiple excitation effect associated with 2p4f at ca. 180 eV above the absorption edge [14]. Also, α phase of PbF_2 has already known to be an asymmetric crystal structure from the viewpoint of Pb atom, thus only structural parameters regarded as averaging 1st coordination shell can be derived by XAFS spectra.

Although these restrictions of XAFS analyses on this system exist, superionic phase transition was clearly observed by indication of drastic phase shifts in XAFS spectra, which is corresponding to rapid increase on dynamics of fluorides [12]. By means of molecular dynamics simulations of PbF_2 at various temperatures using polarizable ionic model [15], the above features at solid phases including superionic phase are well reproduced surprisingly [13]. However, both EXAFS signals and structural parameters of molten PbF_2 are not successfully reproduced by the MD simulation, thus still both efforts on careful re-evaluation of experimental data and potential optimization is required for this system.

In the LiF–PbF_2 mixtures, the structural parameters show 4 fluorides coordinated tetrahedral geometry is predominant except

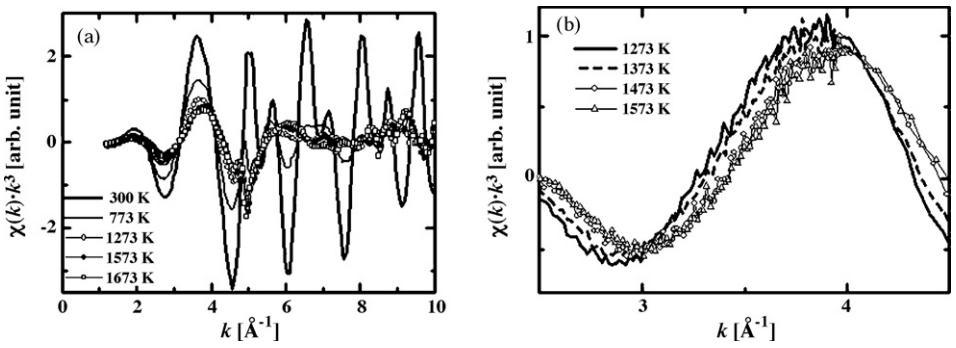

Fig. 1. XAFS oscillations, $\chi(k)\cdot k^3$, of BaF_2 at various temperatures obtained by (a): stepped scan mode (b): quick scanning techniques (in part).

around eutectic composition (it seems to be 6-coordinated predominantly) [13]. These results suggest addition of Li^+ hardly affects on the local structure around Pb^{2+}, since 4-coordinated structure also reported previously in molten PbF_2–KF (x_{PbF2} = 20 mol%) by Raman spectroscopy [16]. This specific feature at eutectic composition may be caused by thermodynamically specific characteristics.

2.2. SrF_2 and its mixture with alkali metal fluorides

Strontium is one of long-lived radioactive fission products, thus local structure around it in molten salt would be valuable information to design a pyrochemical treatment process [17]. SrF_2 is of symmetric fluorite crystal structure at low temperature, and undergoes superionic phase below its melting point (1740 K) [18]. XAFS spectra of pure SrF_2 [19] and mixtures with LiF, NaF, and KF (x_{SrF2} = 20 mol%) at various temperatures have been collected using Sr–K edge. As similar to observation in PbF_2 system, drastic phase shift in XAFS spectra can be identified between 1073 and 1273 K, which is very consistent to superionic phase transition already reported [18]. The structural parameters at molten phase have been carefully evaluated using all temperature conditions, and 4 fluorides coordinated structure which is very close to those observed in superionic phases seems to be stable. For this system, alkali cation species effect have also been studied, but there is no considerable difference among the parameters obtained to be in the range, N_{SrF} = 3.1–3.2 and R_{SrF} = 2.52–2.53 Å at 1173 K. Both values are slightly smaller than those of pure molten SrF_2.

2.3. BaF_2

Barium has been focused also for the same reason above, because it is one of fission products. However the melting point of pure BaF_2 is very high, we used an infrared gold image furnace to heat the sample up to 1673 K under high vacuum condition. The extracted XAFS oscillations, $\chi(k)\cdot k^3$ obtained by stepped scan measurements at various temperatures are shown in Fig. 1(a). Similar to the observation in PbF_2 [12], a small phase shift in EXAFS spectra, corresponding to superionic conduction phase transition, is observed between 1273 and 1573 K. Fig. 1(b) shows the EXAFS spectra obtained by quick-scan technique applied during heating cycle between 1273 and 1573 K. These spectra indicate that the superionic conduction transition occurs between 1373 and 1473 K, and this temperature range lies in-between the superionic transition (1050 K) and melting (1620 K) temperatures reported in [18]. Weaker XAFS signals with continuously overlapped noise, generally lead to ambiguous structural parameters due to several reasons, such as large thermal fluctuations at a given time and/or location causing signal averaging, infrared wave interruption causing non-linearity in ion chambers' counting ability, large current regulated temperature controller causing electrical noise. Also, such high temperature conditions make it difficult to measure temperatures exactly. Thus it becomes essential that further improvements in the design of sample holder and heating device must be carried out. However, the present results indicate that the quick-scan technique would be a promising tool to investigate transient changes even under high temperature conditions.

2.4. Summary of divalent cation metal fluoride systems

One of the most striking results obtained by XAFS analysis for these divalent fluoride systems is that the temperature dependence of the structures has been investigated systematically [20]. As shown in Fig. 2, coordination numbers of fluoride ions around a divalent cation decrease with a temperature increase for all systems. The local structural changes in liquid states of these systems have also been evaluated, and structural properties in

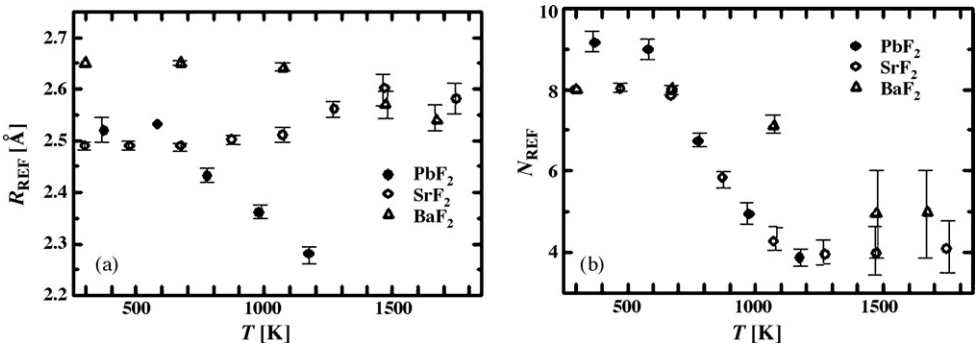

Fig. 2. Temperature dependence of the first coordination structural parameters, i.e., (a) inter-ionic distances and (b) coordination numbers, obtained by XAFS analysis on PbF_2, SrF_2 and BaF_2.

superionic conductor states of fluorite crystals are revealed to resemble liquid structure. In the superionic conductor state of the fluorite crystal, formation of clusters of interstitial anions and vacancies are suggested by neutron diffractions [21]. The XAFS signal of the superionic state is affected stronger by the interstitial anions than fluoride ions at regular lattice positions due to the shorter inter-ionic distances. Therefore, the structural changes in the superionic conductor states are conjectured to be determined by balance of cation-interstitial anion coulombic attraction and thermal diffusing mobility of fluoride ions. Difference in the polarizability of cations would be one of essential factors to lead the local structural difference in divalent fluoride systems.

3. Trivalent cation metal fluorides and their mixtures

3.1. Rare earth metal fluorides

Some of the rare earths are fission products and used as prototypes of nuclear fuel materials. Thus extensive structural analysis on molten fluorides containing rare earths should be necessary to make any materialization of nuclear technology processes.

One of the difficulties in the analysis of XAFS spectra of this system is how to deal with irregular or distinct oscillations caused by multiple electron excitation effects, which is due to 2p4d resonances appeared at ca. $k = 5.7–7$ Å^{-1} [22]. This stepped or spiked feature is especially emphasized under high temperature conditions because the predominant oscillation resulting from coordination structure itself is weakened due to increasing thermal disorder. To show one of the case studies here, we choose XAFS spectra of LaF_3–NaF obtained by using both La–K and La–L_{III} edges [20]. To avoid interruption from multiple electron excitation effects, we utilized another multiple X-ray backscattering simulation code, GNXAS [23]. The detailed analytical procedure has been published [20], but basically, we first perform molecular dynamics (MD) simulations by assuming reasonable inter-ionic pair potential model to obtain average coordination structures, and then input these coordination data into GNXAS code to calculate the XAFS oscillation. The experimentally extracted XAFS oscillations and those calculated from GNXAS code for the La–K and La–L_{III} edges are shown in Fig. 3(a) and (b), respectively. In both cases, the experimental and calculated XAFS oscillations are in good agreement except the spiked features in La–L_{III} spectra. This comparison in *k*-space, thus, validates the inter-ionic potentials used in MD simulations as well as the structural parameters derived from MD. The structural parameters obtained from curve-fitting procedure in *R*-space are slightly underestimated than those derived from MD, thereby showing the limitations of curve-fitting procedure in some cases. However, the S_0^2 value (the reduction factor correlated to the probability of single electron excitation) for La–L_{III} edge data is ca. 0.6, and this implies multiple electron excitation phenomena. This information might be useful in estimating the X-ray excitation probability ratio. It is, thus, not necessarily meaningless to perform curve-fitting analysis on a single peak in *R*-space data.

By following this strategic analysis procedure combined with molecular dynamics simulations, we obtained much reliable local structural information for pure molten rare earth metal fluorides, even though we cannot achieve collection of XAFS spectra on lighter rare earth metal fluorides, e.g., pure LaF_3 due to its high melting point [24]. The 1st coordination distances between rare earth cation and fluoride anion depend directly on ionic size and polarizability of rare earths. The most striking feature is all coordination numbers show more than 6, and 6 fluorides coordinated structures become stabilized toward heavier (smaller cationic sized) elements.

3.2. Mixtures of rare earth metal fluorides and alkali metal fluorides

Although, as illustrated above for pure rare earth fluorides, we need further refinement of XAFS structural parameters in conjunction with MD and diffraction techniques, but the parameters derived for different systems from XAFS spectra can be compared quantitatively with each other to look at the trends in the data. The inter-ionic distances and coordination numbers around M_{II}^{2+} or M_{III}^{3+} ions in pure melts and their mixtures with alkali metal fluorides are plotted versus the elements in Fig. 4(a) and (b), respectively [12,13,19,20,24,25]. Fig. 4(a) indicates perfectly the "lanthanide contraction". The nearest neighbor M_{II}^{2+}–F^- and M_{III}^{3+}–F^- distances have values almost similar to the sum of the ionic radii, M_{II}^{2+} for 4-coordinated structures, $\sigma_{MII} + \sigma_F$, and M_{III}^{3+} for 6-coordinated structures, $\sigma_{MIII} + \sigma_F$ [26]. From this observation, we expect that all the fluoride systems investigated here form on average the 4-coordinated tetrahedra for $M_{II}F_2$ systems and the 6-coordinated octahedra for $M_{III}F_3$ systems in the first coordination shells. Similar observations have earlier been made in chloride and bromide melts [27].

Nevertheless, the trends in the coordination numbers of all the investigated systems seem to be much complicated, especially for the lanthanide fluorides and their mixtures (Fig. 4(b)). But, in general, coordination numbers decrease in mixtures than those in pure melts. Another observation that can be clearly made is that with decreasing ionic radius, the coordination number decreases with the exception of some elements. The dependencies on the type of alkali metal cannot be observed clearly in the case of mixtures with M_IF. Thus, in the investigated concentration region ($x_{MF3} = 20$ mol%), the local environment around lanthanide ion is determined mainly by its own characteristics, i.e., the strong coulombic interactions between M_{III}^{3+} and F^-.

Raman spectroscopy of lanthanide fluoride-potassium fluoride melts suggested that LnF_6^{3-} species are predominant in the molten mixture with alkali fluorides at $xLnF_3 < 25$ mol% [28]. Recent ^{89}Y

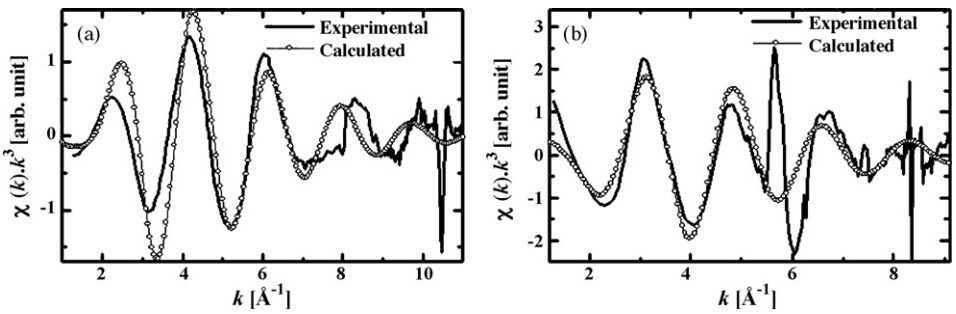

Fig. 3. XAFS oscillations [experimental (lines) and calculated (circles)] of molten LaF_3–NaF ($x_{LaF3} = 20$ mol%) at 1173 K: (a) La–K, (b) La–L_{III} edges.

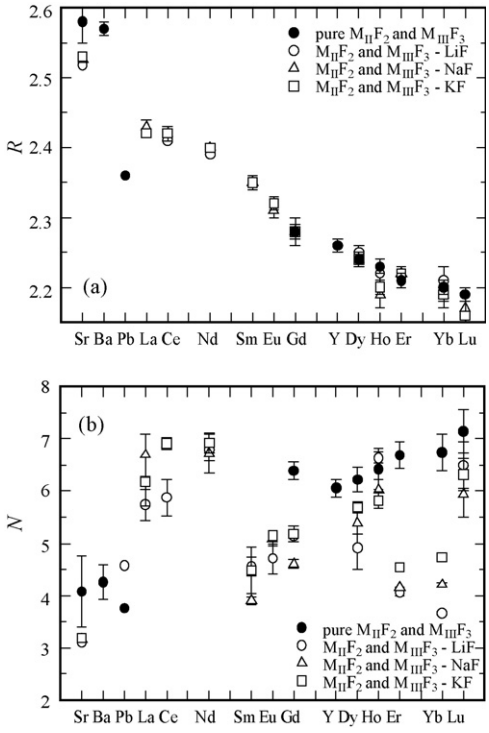

Fig. 4. (a) The inter-ionic distances M_{II}–F and M_{III}–F in molten $M_{II}F_2$ and $M_{III}F_3$, and their mixtures with M_IF, and (b) coordination numbers of these pure melts and mixtures versus M_{II}^{2+} and M_{III}^{3+} ions.

NMR study on YF_3–LiF (x_{YF3} = 30, 50 and 70 mol%) suggested even higher coordination state than octahedra exists in the melts, since all the chemical shift values are very similar to the value of solid $LiYF_4$ (8-coordinated structure) [29]. ^{19}F NMR [29] tells also that free fluoride ions provided by alkali metal fluoride are bound and shared between LnF_x polyhedra at the composition of $xLnF_3 > 25$ mol%, and the number of free fluoride ions decrease with increasing the composition of LnF_3, and then finally a network-like structure is created at pure melt. These discussions lead that the coordination numbers of fluorides around a rare earth ion decrease to 6 by mixing with a large amount of alkali metal fluorides. EXAFS analysis of the systematical study suggests that 4–6-coordination structures dominantly exist in mixture systems at $xLnF_3$ = 20 mol%. Although slight discrepancy can be found in the coordination number, this tendency in concentration dependence obtained by XAFS analysis agrees with the information from already published. Recent ^{139}La NMR study [30] shows clearly the alkali species dependence which does not be identified by EXAFS study. This fact exhibits the limitation of fitting analysis to derive the structural parameters by EXAFS, thus to make precise discussion, combination with other techniques, e.g., NMR and molecular dynamics simulation are important.

4. XAFS experiment and data treatment

4.1. Sample preparation

Although some fluorides are chemically stable enough at room temperature, all the samples have to be treated in a glove box under dried argon circulation from the beginning of sample preparation, since all the fluorides would react with even small amount of oxide at high temperature. For EXAFS measurement, homogeneously distributed samples in X-ray irradiation area have to be prepared to obtain good resolved spectra. One possibility is to confine the molten samples in certain containers with rigid and smooth walls, but it is extremely difficult to find suitable cell materials and design geometry for molten fluorides because of their corrosive nature. Thus the handling technique in which the samples are embedded in inert matrices has been used for molten fluorides measurements as a conventional method. It is the most essential to find inert 'enough' material for matrix. Boron nitride powder (Showa Denko, 99.5% purity, 10 μm particle size on average) has enough stability against molten metal fluoride. Fig. 5 shows B–K (a) and N–K (b) edges X-ray photo emission spectra of the samples used already at high temperature XAFS measurements. In B–K edge spectra, small peaks corresponding to borate can be identified, but they would be negligible on XAFS spectra at high temperature. The other essential issue is to find suitable mixing weight ratios with samples, because if too large ratio of chemicals/BN, samples would immerse out from the matrix, if too less, matrix powder may affect to the local structure of the sample itself. From our experiences, we found suitable chemicals/BN ratio: one pellet of 1/9 for measurements using L_{III} edges, three pellets of 1/4 for measurements using *K* edges and these cover reasonable X-ray absorptions at the X-ray absorption energies for XAFS analysis.

Pure reagents mostly 99.9% or better in purity were used as raw chemicals. In the case of mixtures, the reagents properly weighed were once molten, solidified in glassy carbon crucibles, and ground into powder form with the grain size less than a few μm to get homogeneous mixtures. These reagents were then mixed with BN matrix powder homogeneously for more than half an hour, and pressed into pellets of 13 mm diameter and ca. 1 mm thickness pressured by 10 tons of a mechanical oil hydraulic press and dies. These pellets were installed between two BN sample holders with open windows, and the sample holders were inserted in the rectangle engraved hole of the BN stud to keep the sample vertical to the X-ray irradiation as shown in Fig. 6. French group has also independently developed specific holder for EXAFS measurements at high temperature [31]. The preparation of pellets is in an almost

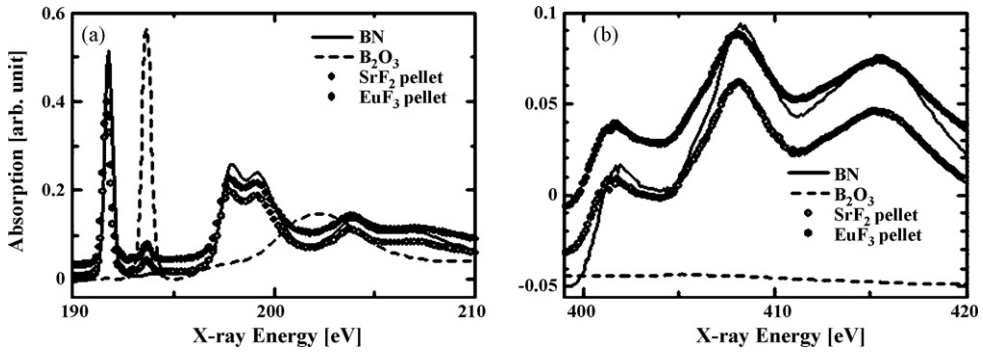

Fig. 5. B–K edge (a) and N–K edge (b) XANES spectra of standard sample (BN and B_2O_3) and used pellet (SrF_2, EuF_3 + BN) for high temperature XAFS measurements.

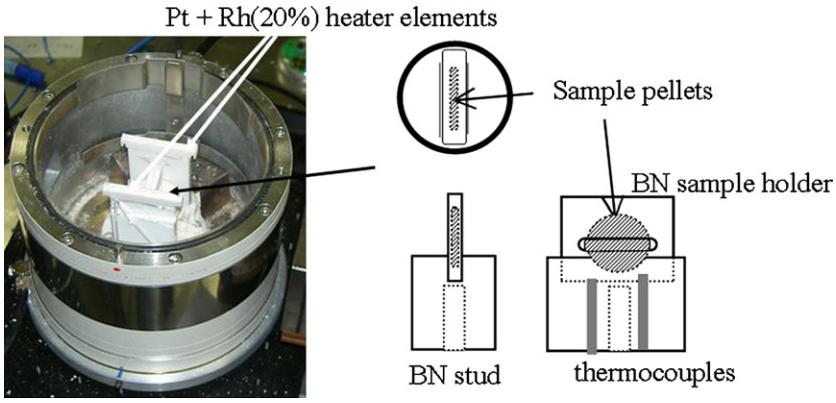

Fig. 6. Inner view of the electric furnace (left) and schematic drawing around the sample pellet (right). BN stud is fixed at middle of the furnace. Two BN plates with holes for X-ray path hold the sample pellet between them, and they are fixed on BN stud as shown in the right figure. Thermocouples inserted from outside of the furnace are fixed in the sample holder just below the pellet (bottom).

similar way, but their holder made from two pyrolytic BN has thin windows at installing part of pellets. Due to larger contact area of two plates, it allows to avoid the effect of outer environment as much as possible. This configuration would be much ideal, especially, for measuring environmentally sensitive samples.

4.2. Furnace

The choice of suitable heating device applicable to XAFS measurements at high temperature is also essential. Required conditions are such that thermal isolation and homogeneous heat distribution around the sample area should be enough achieved; atmosphere can be well controlled; samples can be easily changed; all materials can be easily replaced; and, structure materials should have enough corrosion resistance characteristics specifically for molten fluorides.

The furnace types are categorized into three groups by heating procedures.

(1) Heating element attached directly to the samples: In European Synchrotron Radiation Facility (ESRF), BM29 beamline, the pelleted samples are heated by conducting carbon sheet attached directly to the samples [32]. It is suitable to observe the temperature effect of the sample but it is inadequate for molten fluorides due to their reaction probability with carbon sheet. Also potentially, the furnace chamber is made of glass material that would be easily reacted and, the sample must be kept under high vacuum to establish heat isolation, but deposition of evaporated samples is not negligible if liquid sample has high vapor pressure.

At Conditions Extrêmes Matériaux Haute Température et Irradiation (CEMHTI), a unique furnace has been developed, in which heating elements are made by also graphite plates, but they contact through pyrolytic boron nitride cell [33]. Large contact area would achieve heat homogeneity at the sample.

(2) Heating element non-attached to the samples (resistance): In ESRF BM26, there is another design of a furnace [34]. Heating element is rather simple as like as just bore kanthal heating element rounded by alumina ceramics. But due to complicated structure of furnace including sample installation part, we cannot avoid exposing samples to the atmosphere for a long time, and the most crucial matter is that the furnace itself is not hermetic.

In High Energy Accelerator Research Organization, Photon Factory (KEK-PF), there is a furnace equipped double heaters using sheathed kanthal heating element [35]. This furnace chamber can establish good hermeticity, but due to poor thermal isolation in the chamber, the maximum temperature is limited when the sample should be heated under He gas environment. Also the sample should be inserted from the top which is stuck tightly on the cover, thus usually it takes at least 10 minutes to change the sample.

Thus, we have arranged our own furnace adapted to our purpose. This furnace is designed by Rigaku Corp., shown in Fig. 6. The furnace elements are two alumina plates surrounded by Pt–Rh20% alloy wire and stood at the parallel direction to X-ray. The sufficiently thermal heat homogeneity and isolation is established by using heat shield made of porous silica alumina and well water-cooled aluminium body. The window material of heat shield is either thin nickel foil or aluminium, and the outer windows attached to the body are polyimide films with aluminium coated. The sample pellet with a holder was installed in the central position of the furnace, and the temperature is controlled and monitored by two R-thermocouples inserted from the bottom of the furnace within ± 5 K of the set value after equilibrium. This furnace environment can be well controlled either under gas flowing or vacuum using a rotary pump. The most advantage of this furnace is in the simple construction, and we can thus quickly change the samples and repair it if we meet something trouble.

Japan Atomic Energy Agency has also independently developed the furnace, which is constructed by cylindrical furnace element surrounded by kanthal wire, and water-cooled stainless steel body [27]. It has been devoted only to molten chloride studies.

(3) Heating element non-attached to the samples (others): To achieve much higher temperature than that produced by a resistance furnace, we have also experienced to develop infrared gold image furnace system. Basically, it is constructed by commercial equipment (ULVAC Inc.) using Tungsten heater lamps to emit the infrared. However, to protect oxidation from the heat from these lamps, we have to introduce not only cooling system by water for entire body, but also air compressed to cool directly these heater elements themselves. Furthermore, the sample should be kept in the transparent quartz chamber under high vacuum achieved by a turbo molecular pump. As described previously, the technical problems still exist in the application of this system to heat fluorides; e.g., to optimize the sample holder to avoid damaging by heat from the sample irradiated, and to protect the ionic chambers to be affected by the infrared radiation from the furnace itself.

4.3. XAFS measurement

The optics and setups of XAFS measurement can be utilized without any modification as can be provided by the beamlines in any central synchrotron facilities [32,35,36]. The monochromatized X-rays were cut by two-dimensional slit adjusted to be irradiated in the sample target area, in our case, e.g., 1 mm high and 2–5 mm wide. The sample in the furnace should be kept fixed between two ionic chambers to monitor X-rays, one for incident and the other for transmitted. The most important thing when we install the furnace in the beamline is that any inhomogeneous material should not interrupt an X-ray beam. Usually, an x–z mechanical stage or a lab-jack to monitor with X-ray sensitized paper or sheet was used for sample geometry alignment, and sometimes an automatic stage to monitor X-ray image of transmitted beam with X-ray CCD camera also can be used. However, even though we thought the all optics and furnace geometries were completed in exactly the same way, sometimes, we notice the difference in the quality of XAFS spectra using exactly the same samples in the same temperature conditions in the different time. Thus, if we want to compare the XAFS spectra with each other much precisely, it is ideal to collect the systematic data in the same time.

The XAFS spectra discussed above have been collected systematically by using beam lines BL7C (La–L_{III}, Ce–L_{III}, Nd–L_{III}, Sm–L_{III}, Gd–L_{III}, Dy–L_{III}), BL10B (Pb–L_{III}, Er–L_{III}, Yb–L_{III}), BL27B (Sr–K, Y–K, Eu–L_{III}, Ho–L_{III}, Lu–L_{III}) at the KEK-PF (Japan), and on beam lines BL01B1 (Ba–K), BL16B2 (La–K, Sm–K), BL38B1 (Ce–K, Sm–K) at the SPring-8 (Japan). The X-rays used for measurement are obtained by double crystals of Si (1 1 1) monochromatized with detuned at PF BL7C and BL27B, channel cut single crystal of Si (3 1 1) monochromatized at PF BL10B and double crystals of Si (3 1 1) monochromatized with Rh coated focusing mirrors to prevent from contamination of higher ordered X-ray at SPring-8. The gases for ionic chambers depend on the X-ray energies and the size of ionic chamber ideally, but usually, we chose them depending upon measured energy ranges, $E < 10$ keV for I_0: N_2, I: Ar + N_2, $E > 10$ keV for I_0: Ar + N_2, I: Ar, $E > 30$ keV for I_0: Ar + Kr, I: Kr. In normal step-scanning method, the counts of I_0 and I are collected for 1 s at each energy step: 4.0, 1.0, 2.0 and 4.0 eV for the appropriate energy ranges to cover enough oscillation for solid phase (k = ca. 18 Å^{-1}). In order to take into account the statistical errors in the data, an average of at least five consistent scans were used for the final data analysis.

4.4. Data analysis: cumulant fitting

Since the analytical procedure of XAFS spectra by using WinXAS 2.3 software [37] has already been written in detail [20], we describe briefly about the most essential part in this review. The modified Victoreen equation with three fitting parameters was used for the pre-edge energy region and the fitted curve was subtracted from the whole spectrum to obtain background-subtracted spectrum at first. Secondly, it was divided by edge jump height to obtain the normalized spectrum. Third, to convert the energy to k^{-1}, the absorption threshold energy, E_0 was decided by the inflection point on the edge jump. And then, XAFS signal, $\chi(k)$ was extracted from the background-corrected X-ray absorption spectrum by assuming that the X-ray absorption of isolated absorber was expressed as a combination of three 2nd degree polynomials. Radial structure function, $\mathrm{FT}|\chi(k)\cdot k^3|$ was obtained by Fourier transformation of k^3-weighted XAFS oscillation. However, this radial structure function does not represent the radial distribution function since the inter-ionic correlation peak appears normally at the slightly shorter position from the correct inter-ionic distance. Thus, theoretical calculation of backscattering factors and peak fitting analysis are necessary to obtain the quantitative structural information. The backscattering amplitude and the phase shift used for fitting analysis were derived from the theoretical calculation of multiple X-ray scattering by FEFF 8.0 XAFS simulation code [38]. Local structural parameters around each multivalent ion were derived by curve-fitting analysis applied to the first neighboring M_{II}^{2+}/M_{III}^{3+}–F^- correlation peak in $\mathrm{FT}|\chi(k)\cdot k^3|$. Correction terms related to the unharmonic oscillation effects, 3rd and 4th cumulants should be introduced in the fitting parameters at high temperatures. Structural parameters such as coordination number, Debye Waller factor, 4th cumulant factor and inter-ionic distance, E_0 shift, 3rd cumulant factor are highly correlated one another. Thus, the spectra at various temperatures were utilized to derive physically reasonable structural parameters. To reduce uncertainty of parameter fitting procedure, we also have utilized thermally equilibrated ionic configurations derived by molecular dynamics simulations to reproduce XAFS spectra using either repeating FEFF calculation [39] or GNXAS code [23] in some cases.

5. Concluding remarks

As we explained above, structural parameters such as the inter-ionic distances and the nearest neighbor coordination numbers of fluoride ions around multivalent ions were systematically obtained by XAFS analyses.

XAFS is a powerful tool to elucidate local structures of materials at high temperatures and transient states, and its applicability to a variety of systems would be still opened, e.g., to obtain the structural information on the systems containing nuclear materials and to elucidate the mechanism of in situ electrochemical and/or reduction–oxidation reaction to follow the time and space variations. For these purposes, the technical innovation on both X-ray optics and sample environment would be still needed and underdeveloped, thus quick scanning, micro-beam, and fluorescence measurement techniques combined with high energy X-rays are surely expected. Also, the analytical procedure of XAFS can be further refined. One of the possibilities of structural refinement procedure is aided by MD simulations with PIM + FEFF [39], but in several cases, XAFS spectra could not be well reproduced yet by using empirical pair potentials. To focus on the alkali dilution effect, French group has accumulated XAFS spectra of LiF–LaF_3, LiF–YF_3, LiF–LuF_3 and LiF–ThF_4 at high temperatures by combination with NMR spectroscopy [40]. These are quite valuable data which would contribute to draw a global model for mixtures, but quantitative analyses are underway. To obtain further firm structural parameters that would stand the test of time, XAFS technique should be used in conjunction with numerical calculations, and extra efforts to accumulate structural information from X-ray and neutron diffractions as well as spectroscopic techniques should be made. Such multi-technique approaches should also pave the way to construct a generic model for MD simulations and to expect chemical behavior at practical pyrochemical reprocessing processes.

Acknowledgements

We wish to thank Drs. M. Matsuzaki, T. Sakamoto, Messers A. Nezu, R. Toyoyoshi, K. Naoi, T. Kanuma, M. Hatcho, N. Kitamura, T. Ichiki, S. Kakizaka at Tokyo Tech. for the experimental assistance. XAFS experiments have been carried out with the approval of the Photon Factory Program Advisory Committee (Proposal Nos. 2001P015, 2002G080, 2002G281, 2003G084, 2004P006, 2004G064, 2004G080, 2004G303), SPring-8 (2002B0541-NX-np,

2004A0546-NXa-np, 2004A0548-NI-np, C04A16B2-4050-N, 2004B0668-NXa-np) and cooperative research program between Tokyo Tech. and JAERI. We are also grateful to the JSPS for the financial support for the Joint Project between the Japan and UK partners under the "Japan-UK Research Cooperative Program", 99GC0006. HM expresses acknowledgment to Drs. C. Bessada and A.–L. Rollet for valuable up-to-date information of structural analyses and encouragement of this article written up.

References

[1] S.K. Oh, K.M. Chung, Nucl. Eng. Des. 207 (2001) 11–19;
J.-M. Loiseaux, S. David, D. Heuer, A. Nutin, C. R. Phys. 3 (2002) 1023–1034;
U. Gat, J.R. Engel, Nucl. Eng. Des. 201 (2001) 327–334.
[2] M. Matsumiya, H. Matsuura, J. Electroanal. Chem. 579 (2005) 329–336.
[3] A. Sagara, O. Motojima, O. Mitarai, S. Imagawa, K. Watanabe, H. Yamanishi, H. Chikaraishi, A. Kohyama, H. Matsui, T. Muroga, N. Noda, T. Noda, N. Ohyabu, T. Satow, A.A. Shishkin, S. Tanaka, T. Terai, K. Yamazaki, J. Yamamoto, F.F.H.R. Group, J. Nucl. Mater. 248 (1997) 147–152.
[4] M. Ablanov, H. Matsuura, R. Takagi, J. Nucl. Mater. 258–263 (1998) 500–504.
[5] T. Mukaiyama, T. Takizuka, M. Mizumoto, Y. Ikeda, T. Ogawa, A. Hasegawa, H. Takada, H. Takano, Prog. Nucl. Energy 38 (2001) 107–134.
[6] L.M. Toth, A.S. Quist, G.E. Boyd, J. Phys. Chem. 77 (1973) 1384–1388.
[7] B. Gilbert, G. Mamantov, G.M. Begun, Appl. Spectrosc. 29 (1975) 276–278;
F. Auguste, C. Bessada, B. Gilbert, in: Proceedings of Symposium on Molten Salt Chemistry and Technology, 7, 2005, pp. 51–58.
[8] V. Dracopoulos, B. Gilbert, B. Borrensen, G.M. Photiadis, G.N. Papatheodorou, J. Chem. Soc., Faraday Trans. 93 (1997) 3081–3088;
V. Dracopoulos, J. Vagelatos, G.N. Papatheodorou, J. Chem. Soc., Dalton Trans. 2001 (2001) 1117–1122.
[9] V. Lacassagne, C. Bessada, P. Florian, S. Bouvet, B. Ollivier, J.-P. Coutures, D. Massiot, J. Phys. Chem. 106 (2002) 1862–1868;
I. Nuta, C. Bessada, E. Veron, G. Matzen, C. R. Chim. 7 (2004) 395–400.
[10] F. Lytle, J. Sychrotron Rad. 6 (1999) 123–134;
D. Sayers, F. Lytle, E. Stern, Adv. X-Ray Anal. 13 (1970) 248–271.
[11] L. Ehm, K. Knorr, F. Mädler, H. Voigtländer, E. Busetto, A. Cassetta, A. Lausi, B. Winkler, J. Phys. Chem. Solid 64 (2003) 919–925;
I. Kosacki, Appl. Phys. A49 (1989) 413–424.
[12] S. Watanabe, R. Toyoyoshi, T. Sakamoto, Y. Okamoto, Y. Iwadate, H. Akatsuka, H. Matsuura, J. Phys. Chem. Solids 66 (2005) 402–405;
S. Watanabe, R. Toyoyoshi, T. Sakamoto, Y. Okamoto, Y. Iwadate, H. Akatsuka, H. Matsuura, Phys. Scr. T115 (2005) 297–301.
[13] S. Watanabe, H. Matsuura, H. Akatsuka, Y. Okamoto, P.A. Madden, J. Nucl. Mater. 344 (2005) 104–108.
[14] A. Di Cicco, A. Filipponi, Phys. Rev. B 49 (1994) 12564–12571.
[15] M.J. Castiglione, M. Wilson, P.A. Madden, C.P. Grey, J. Phys. Condense Matter. 13 (2001) 51–66.
[16] G.N. Papatheodorou, in: Proceedings of Sixth International Symposium on Molten Salt Chemistry and Technology, Shanghai, (2001), pp. 28–35;
V.D. Dracopoulos, Th. Kastrissios, G.N. Papatheodorou, J. Non-Cryst. Solids 351 (2005) 640–649.
[17] K. Nagakubo, H. Matsuura, R. Takagi, Denki Kagaku (Electrochemistry) 63 (1995) 938–940.
[18] B.M. Voronin, S.V. Volkov, J. Phys. Chem. Solids 62 (2001) 1349–1358.
[19] S. Watanabe, Y. Okamoto, K. Minato, H. Akatsuka, H. Matsuura, Electrochemistry 73 (2005) 617–619.
[20] S. Watanabe, Doctor Thesis, Tokyo Institute of Technology (2006).
[21] H.L. Tuller, M. Balkanski (Eds.), Science and Technology of Fast Ion Conductors, Plenum, New York, 1987, pp. 167–196.
[22] J.A. Solera, J. Garcia, M.G. Proietti, Phys. Rev. B 51 (1994) 2678–2686.
[23] A. Filipponi, A. Di Cicco, Task Quarterly 4 (2000) 575–669.
[24] S. Watanabe, A.K. Adya, Y. Okamoto, H. Akatsuka, H. Matsuura, J. Indian Chem. Soc. 82 (2005) 1059–1063.
[25] S. Watanabe, A.K. Adya, Y. Okamoto, N. Umesaki, T. Honma, H. Deguchi, M. Horiuchi, T. Yamamoto, S. Noguchi, K. Takase, A. Kajinami, T. Sakamoto, M. Hatcho, N. Kitamura, H. Akatsuka, H. Matsuura, J. Alloys Compd. 408–412 (2006) 71–75.
[26] R.D. Shannon, Acta Cryst. A 32 (1976) 751–767.
[27] Y. Okamoto, H. Shiwaku, T. Yaita, H. Narita, H. Tanida, J. Mol. Struct. 641 (2002) 71–76.
[28] V. Dracopoulos, B. Gilbert, G.N. Papatheodorou, J. Chem. Soc., Faraday Trans. 94 (1998) 2601–2604.
[29] C. Bessada, A.-L. Rollet, A. Rakhmatullin, I. Nuta, P. Florian, D. Massiot, C. R. Chim. 9 (2006) 374–380.
[30] A.-L. Rollet, S. Godier, C. Bessada, Phys. Chem. Chem. Phys. 10 (2008) 1–7.
[31] A.-L. Rollet, C. Bessada, Y. Auger, P. Melin, M. Gailhanou, D. Thiaudiere, Nucl. Instr. Met. Phys. Res. B 226 (2004) 447–452.
[32] A. Filipponi, A. Di Cicco, Nucl. Inst. Met. Phys. Rev. B93 (1994) 302–310; http://www.esrf.eu/UsersAndScience/Experiments/XASMS/BM29/
[33] C. Bessada, A. Rakhmatullin, A.-L. Rollet, D. Zanghi, J. Nucl. Mater. 360 (2007) 43–48.
[34] http://www.esrf.eu/UsersAndScience/Experiments/CRG/BM26/Xafs.
[35] http://pfwww.kek.jp/nomura/pfxafse/.
[36] http://www.spring8.or.jp/wkg/BL01B1/instrument/lang-en/INS-0000000375/instrument_summary_view.
[37] T. Ressler, J. Phys. IV 7 (1997) C2–269;
T. Ressler, J. Synch. Rad. 5 (1998) 118–122.
[38] S.I. Zabinsky, J.J. Rehr, A. Ankudinov, R.C. Albers, M.J. Miller, Phys. Rev. B 52 (1995) 2995–3009.
[39] Y. Okamoto, Nucl. Inst. Met. Phys. Res. A 526 (2004) 572–583.
[40] A.-L. Rollet, C. Bessada, A. Rakhmatoulline, Y. Auger, P. Melin, M. Gailhanou, D. Thiaudiere, C. R. Chim. 7 (2004) 1135–1140;
A.-L. Rollet, A. Rakhmatullin, C. Bessada, Int. J. Thermodyn. 26 (2005) 1115–1125.